Biomed. Mater. **2** (2007) 67–77 doi:10.1088/1748-6041/2/2/003

Osteoblast proliferation on hydroxyapatite thin coatings produced by right angle magnetron sputtering

A Mello[1,2], Z Hong[3], AM Rossi[2], L Luan[3], M Farina[4], W Querido[4], J Eon[5], J Terra[2], G Balasundaram[6], T Webster[6], A Feinerman[7], D E Ellis[3], J B Ketterson[3] and C L Ferreira[1]

[1] Instituto Militar de Engenharia, IME, Rio de Janeiro, 22290-270, RJ, Brazil
[2] Centro Brasileiro de Pesquisas Físicas, Rua Dr. Xavier Sigaud, 150, Rio de Janeiro, 22290-180, RJ, Brazil
[3] Department of Physics and Astronomy, Northwestern University, Evanston, IL 60208, USA
[4] Instituto de Ciências Biomédicas, Universidade Federal do Rio de Janeiro, Ilha do Fundão, Rio de Janeiro, RJ, 21941-590, Brazil
[5] Inst. Química, PUC/RJ, Rio de Janeiro, 21941-590, RJ, Brazil
[6] Division of Engineering, Brown University, Providence, RI, 02912, USA
[7] Department of Electrical and Computer Engineering, University of Illinois, Chicago, IL, 60612, USA

E-mail: mello@cbpf.br, hong@northwestern.edu and j-ketterson@northwestern.edu

Received 8 December 2006
Accepted for publication 5 February 2007
Published 14 March 2007
Online at stacks.iop.org/BMM/2/67

Abstract
Right angle magnetron sputtering (RAMS) was used to produce hydroxyapatite (HA) film coatings on pure titanium substrates and oriented silicon wafer (Si(0 0 1)) substrates with flat surfaces as well as engineered surfaces having different forms. Analyses using synchrotron XRD, AFM, XPS, FTIR and SEM with EDS showed that as-sputtered thin coatings consist of highly crystalline hydroxyapatite. The HA coatings induced calcium phosphate precipitation when immersed in simulated body fluid, suggesting *in vivo* bioactive behavior. *In vitro* experiments, using murine osteoblasts, showed that cells rapidly adhere, spread and proliferate over the thin coating surface, while simultaneously generating strong in-plane stresses, as observed on SEM images. Human osteoblasts were seeded at a density of 2500 cells cm^{-2} on silicon and titanium HA coated substrates by RAMS. Uncoated glass was used as a reference substrate for further counting of cells. The highest proliferation of human osteoblasts was achieved on HA RAMS-coated titanium substrates. These experiments demonstrate that RAMS is a promising coating technique for biomedical applications.

1. Introduction

Stainless steel, titanium and titanium alloys are used worldwide in orthopedic clinical procedures for bone substitution and repair because of their superior mechanical properties and biocompatibility [1, 2]. In spite of their intensive use in such applications, sustained efforts have been made over the last two decades to improve their surface bioactivity and compatibility. Research in this field has mainly focused in two directions: (i) developing mechanical and chemical treatments to activate the metal surface bioactivity [3, 4]; and (ii) covering the metal surfaces with a suitably active biomaterial, such as hydroxyapatite. Both approaches have been used in commercial implants of titanium but a complete solution to this problem is still far from being achieved. In general, the titanium surface is treated mechanically and chemically in order to give it an appropriate texture and/or to produce new chemical species on the surface that improve the tissue bonding. On the other hand, the majority of the commercially coated implants utilize a plasma spraying technique to bind hydroxyapatite to the metal surface [5, 6]. The plasma spray coating procedure is fast, inexpensive and

produces reasonably adherent calcium phosphate coatings on the metal surfaces. However, it involves a high-temperature process which causes the coatings to be inhomogeneous and also induces multiple mineral phases, being some of them amorphous. This contributes to instability and degradation of the implant. In order to overcome these limitations, and produce coatings with controlled stoichiometry and crystallinity, several techniques have been developed recently using biomimetic methods [7], electrochemical deposition [8], sol-gel [9], ion-beam assisted deposition [10, 11], electron-beam evaporation [12], laser assisted deposition [13] and magnetron sputtering [13, 14].

Several papers have demonstrated that radio frequency (at 13.56 MHz) magnetron sputtering (RFMS) is a promising technique having the following advantages: high depositing rates, relatively low deposition temperatures, good thickness control, better adhesion between coating and substrate and improved control over coating stoichiometry [15, 16]. However, the as-sputtered coating is usually not crystalline and requires a post-deposition heat treatment to transform the amorphous calcium phosphate phases into crystalline hydroxyapatite [17–21].

It is well known that magnetron sputtering in the presence of oxygen also results in a bombardment of the substrate with positive argon ions attracted by the negative oxygen ions which, in turn, results in preferential back-sputtering of already-deposited material, and both alters the chemical composition, causing degradation of the crystallinity. The result is that an amorphous contribution is predominant and thermal treatments at high temperatures (800 °C) are necessary to induce crystalline phases. This additional treatment increases the cost of the coating process and may result in loss of coating adhesion to the substrate due to different thermal stress.

In depositing thin films of oxide-based superconductors it was early discovered that superior films could be prepared (with respect to crystallinity and chemical composition) by setting the substrate at right angles relative to, and to the side of, the sputter-gun axis; although this produced superior films, the deposition rates (and target utilization) suffered badly. Our group has developed an arranging of *two* sputtering guns back-to-back. By setting again the substrate and gun axes at right angles, superior HA films and much higher deposition rates could be achieved [22].

Here we demonstrate that the right angle magnetron sputtering (RAMS) geometry also produces superior HA films. This is confirmed by synchrotron x-ray diffraction (SXRD) studies which show that HA is the only crystalline phase present in the as-sputtered thin coating and that the HA film crystallinity is comparable to stoichiometric HA powder sintered at temperatures higher than 1100 °C. Coatings with such characteristics were produced by RAMS on silicon and titanium substrates with both flat and engineered (machined and patterned) surfaces. The coatings were then immersed in simulated body fluid (SBF) and the formation of a new calcium phosphate precipitate on the coating surface was observed. In addition, murine osteoblast cells were seeded onto flat and engineered coatings and the behavior of cells on these different surfaces was analyzed by scanning electron microscopy (SEM). Finally we compared the human osteoblast proliferation rate of a reference substrate with that of HA coatings produced by RAMS over silicon and titanium substrates.

2. Materials and methods

2.1. Target and substrate preparation

Hydroxyapatite targets were prepared by uniaxially pressing powdered stoichiometric HA under 30 MPa. Discs 25 mm in diameter and approximately 3 mm thick were then sintered at 1100 °C for 2 h. Substrates were cut from polycrystalline titanium sheet and (0 0 1) silicon single crystal wafers. All the samples were ultrasonically cleaned with acetone, washed in deionized water, immersed in a solution of hydrofluoric acid 10% v/v for 10 min [23]. After that, they were washed in deionized water, and dried under high pressure nitrogen flow. All the sample preparation steps were performed in a laminar flow hood.

2.2. Opposing magnetron sputtering system and film deposition

The opposing magnetron sputtering system consisted of two water-cooled sputtering guns facing each other. The magnetic field was provided by cylindrical neodymium iron boride permanent magnets located inside the copper electrode of each gun (where the water flows); these magnets were oriented such that the magnetic field was maximal in the space between the guns where the plasma was concentrated. The guns were attached to the sputtering chamber, which is a commercial six-way cross with a volume of about 1 l, via quick-connect vacuum flanges. The two opposing HA targets were bonded to thin permalloy (NiFe) discs which were held against the gun electrodes by the field generated by the gun magnets. The substrate holder was positioned at right angles to the two targets at a distance of about 18 mm [24].

In all the experiments the sputtering gas used was a mixture of ultra-high purity oxygen and argon with partial pressures set at 6.66×10^{-1} Pa (5.0 mTorr) and 1.33×10^{-1} Pa (1.0 mTorr), respectively. The RF power varying from 100–130 W was applied to the two opposing targets through an impedance matching pi-network. Special precautions were taken in order to remove contaminants from the chamber and targets. Before initiating the sputtering process, the chamber was evacuated with a turbo pump to a base pressure lower than 1.33×10^{-4} Pa (10^{-6} Torr). The chamber gas species (including the injected oxygen and argon) were continuously monitored using a residual gas analyzer (RGA). A pre-sputtering of the targets was carried out before every deposition. During this process the substrate was protected from contamination by a shutter placed between the targets and the substrate. Under the ambient conditions the temperature of the substrate holder rose to around 60 °C. The maximum deposition time used in this work was 3 h.

Two series of films were prepared under the same conditions. One series was prepared for structural

characterization and the other for bioactivity and cell culture studies. The first series utilized RF powers of 100 W, 120 W and 130 W and deposition times of 2.5, 15, 30, 60 and 180 min. After the XRD, FTIR and XPS analyses, the first series of films were annealed at 400 and 600 °C for comparative studies.

Calcium phosphate coatings were deposited on Si and Ti substrates for cell culture studies. In one group HA was deposited on half of the Si surface while the other half was covered. We refer to the region coated with an HA layer as 'HA/Si', and the other side (with a native silicon surface) as 'Si/Si'. Similar samples were prepared on Ti substrates with HA deposited on one half with the remaining half bare; we refer to the HA covered region as 'HA/Ti', and the bare Ti side on the same substrate as 'Ti/Ti'. We will call substrates prepared in this way *biphasic*.

For cell culture experiments, HA coatings were either sputter deposited onto micro-grooved silicon substrates (groove width = 68 μm, step width = 38 μm, groove depth = 100 μm) to form a 'step and groove' pattern; or photolithographically patterned after deposition using hydrochloric acid as an etchant, to generate a 'cylindrical pillar' pattern (diameter = 60 μm, height = 1 μm)

2.3. Film characterization

Film thickness was measured with a Tencor P-10 surface profiler (KLA-Tencor, CA, USA). X-ray powder diffraction (XRD) was performed using synchrotron radiation (at the Brazilian Synchrotron Light Laboratory: LNLS/Campinas/Brazil) to investigate mineral phases, degree of crystallinity and preferential orientation of the films. The XRD patterns were recorded at a beamline energy of 9.0 kV ($\lambda = 1.377$ Å) and scanned in steps of $2\theta = 0.05°$, in the range 5–60° at a dwell time of 2 s per step.

Diffuse reflectance infrared Fourier transform spectroscopy (DRIFTS) experiments were performed using a Thermo Nicolet Nexus 870 FTIR spectrometer with a Tabletop optics module. The spectra were collected over a range of 400–4000 cm^{-1} with a resolution of 4 cm^{-1} and averaged over 256 scans to characterize the phosphate, hydroxyl and carbonate functional groups.

X-ray photoelectron spectroscopy (Omicron ESCAPROBE, Taunusstein, Germany) was used to determine the film surface composition. All surface spectra were obtained over the range of 0–1000 eV. When operating at an anode voltage of 15 kV and an emission current of 20 mA with the Al Kα source, the x-ray penetration depth is less than 100 Å. The Ca/P ratio was extracted from the ratio of the corresponding integrated peak area after removal of the linear background; the sensitivity factors of the two elements were obtained beforehand by calibrating with powder samples of known composition.

Atomic force microscopy (AFM) images were obtained in the tapping mode with a digital instruments (Santa Barbara, CA) nanoscope atomic force microscope.

2.4. In situ calcium phosphate formation in simulated body fluid (SBF)

A film deposited for 3 h at 120 W was kept in a SBF solution (for details see Takadama *et al* [25]) for 10 days in order to estimate the film capacity for stimulating the formation of a calcium phosphate deposit on its surface.

2.5. Cell culture

2.5.1. Experiments for murine cells growth behavior. Cells were isolated from the endosteal region of a Balb/c mouse femur by using enzymatic digestion (for details see Balduino *et al* [26]), and seeded onto the substrates in order to assess the growth behavior of the osteoblasts on surfaces whose topography and chemistry are well known. Approximately 2.0×10^4 osteoblasts in DMEM (Dubelcco's modified Eagle medium), supplemented with 10% bovine fetal serum, were seeded and the whole assembly was incubated at 37 °C under 5% CO_2.

For seeding, a small drop of the medium containing the cells was deposited on the surface to be studied in specific regions (e.g., part of the drop covering a HA/Si or HA/Ti and the other part over the Si/Si or Ti/Ti region, respectively).

After growth times of 3 h, 24 h, 48 h and 72 h, the samples were fixed in glutaraldehyde 2.5% in 0.1 M sodium cacodilate buffer for about 2 h. Thus, they were washed in the buffer, postfixed for 30 min in 1% OsO_4 in the same buffer and washed again. Afterwards, they were dehydrated in a graded series of ethanol, critical point dried with CO_2, and sputter coated with gold in a Balzers apparatus. Analysis of the samples was performed in a JEOL 5310 scanning electron microscope operated at 20 kV.

2.5.2. Experiments using human osteoblasts. For these cell culture studies, uncoated glass was used as a reference substrate. All substrates were sterilized under UV light exposure for 4 h prior to the cell experiments. Human osteoblasts (bone-forming cells; CRL-11372 American Type Culture Collection, population numbers 7–8) in Dulbecco's modified Eagle medium (Gibco) supplemented with 10% fetal bovine serum (Hyclone) and 1% penicillin/streptomycin (Hyclone) were seeded at a density of 2500 cells cm^{-2} onto the compacts of interest and were then placed in standard cell culture conditions (that is, a humidified, 5% CO_2/95% air environment) for 4 h. After the prescribed time period, substrates were rinsed in phosphate buffered saline to remove any non-adherent cells. The remaining cells were fixed with formaldehyde (Aldrich Chemical Inc., USA), stained with Hoescht 33258 dye (Sigma), and counted under a fluorescence microscope (Zeiss Axiovert 200M). Five random fields were counted per substrate. All experiments were run in duplicate. Standard *t*-tests were used to check statistical significance between means.

In vitro experiments using both murine and human osteoblast cells have followed the international guidelines for care and use of animal cells.

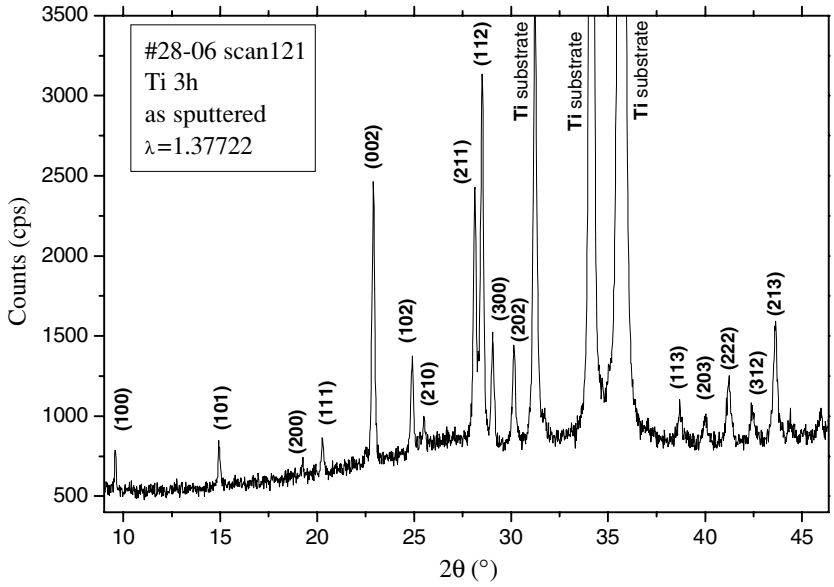

Figure 1. Synchrotron x-ray diffraction pattern of an as-sputtered HA film on Ti substrate for sputtering time of 180 min with 120 W RF power.

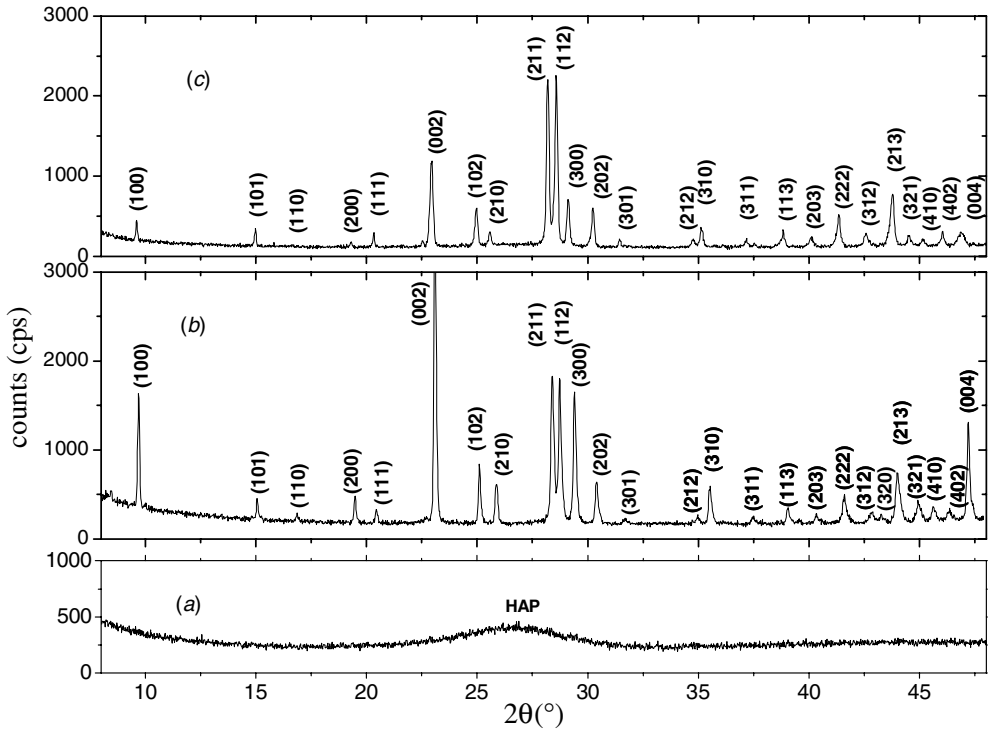

Figure 2. Synchrotron x-ray diffraction pattern of HA films on Si(0 0 1) substrate for sputtering time of 180 min: (*a*) as-sputtered with 100 W RF power; (*b*) annealed at 400 °C after sputter deposition with 100 W RF power; (*c*) as-sputtered with 120 W RF power.

3. Results

3.1. Film preparation and characterization

Calcium phosphate films were produced on silicon (0 0 1) and on titanium substrates using different RF powers and sputtering times. These parameters were varied in order to determine the best condition to form stoichiometric and crystalline hydroxyapatite on the substrate surface without the interference of additional calcium phosphate phases. It was observed that film crystallinity was very sensitive to RF power. As shown in figures 1 and 2(*c*), as sputtered crystalline HA films were obtained for RF powers higher than 100 W. High qualities HA coatings were obtained on both substrates for sputtering times of 180 min with 120 W RF power. Under these conditions the thickness of the coating was about 500 nm. For shorter sputtering times (thickness $<$ 300 nm) stoichiometric hydroxyapatite was also produced, however the

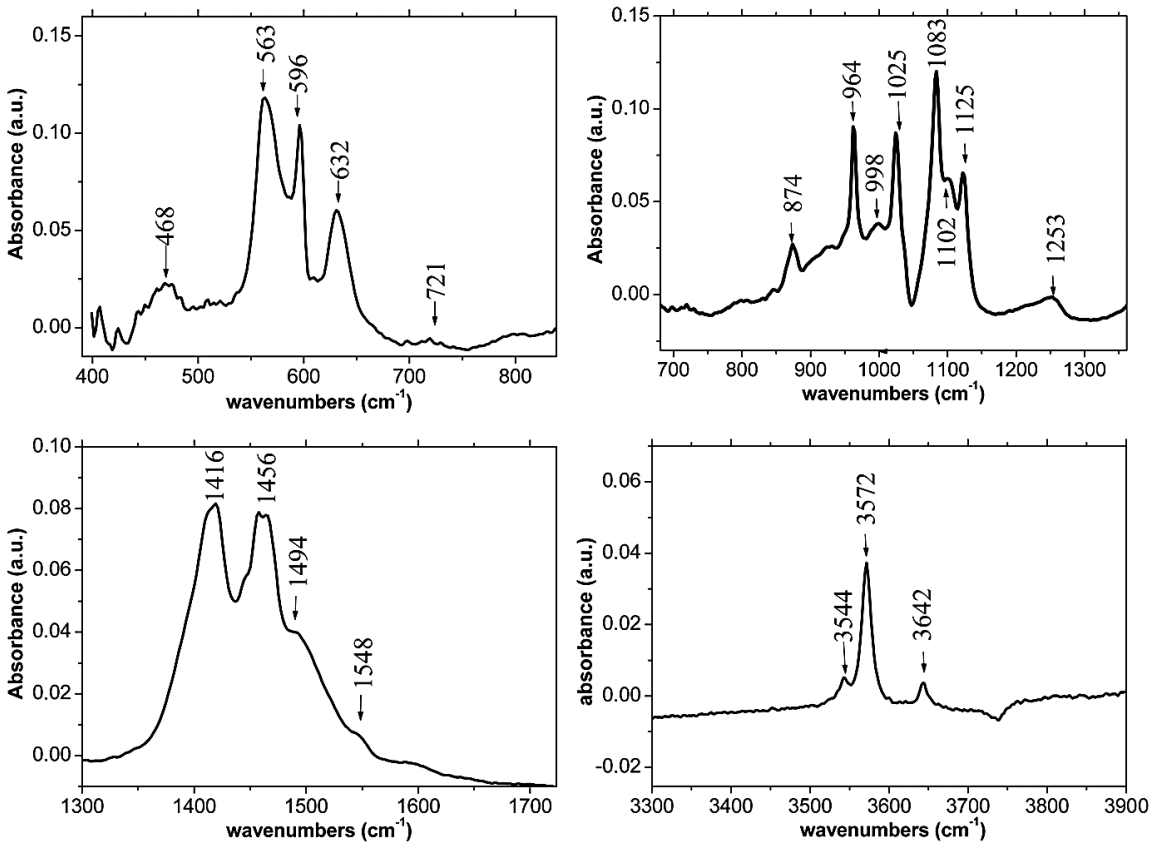

Figure 3. FTIR spectra of as-sputtered HA films on silicon substrate for sputtering time of 180 min with 120 W RF power.

films were highly amorphous. In these cases crystallinity could be improved by heat treating the samples at a moderate temperature (lower than 500 °C) as shown in figure 2(*b*).

The XRD pattern of 180 min and 120 W films on Ti and Si(0 0 1) substrates are shown in figures 1 and 2(*c*) respectively. All HA peaks were identified and the amorphous contribution was very small. The HA peaks have 0.1° linewidth which is smaller (corresponding to more crystalline material) than the HA powder annealed at 1100 °C. A thermal treatment at 400–600 °C did not improve the crystallinity of 180 min films on Si(0 0 1) and Ti substrates as determined from the linewidth observed on the XRD patterns. However, the thermal treatments contributed to a preferential orientation along the HA *c* axis direction [0 0 2] (figure 2(*b*)) when applied to the previously amorphous 100 W film, as shown in figure 2(*a*).

The XRD results were supported by measurements of FTIR spectroscopy. The main FTIR bands for films sputtered for 3 h are characteristic of well crystallized HA. The HA band at 3570 cm^{-1} and at 630 cm^{-1} is strong and narrow, indicating that the OH sites are well ordered. The same behavior is seen with PO_4^{3-} bands in the 1000 cm^{-1} and 500 cm^{-1} region, which are more resolved than the bands of a powdered HA sample after thermal treatment at high temperatures, as shown in figure 3. The above results are clear evidence that magnetron sputtering in the right angle geometry can produce highly crystalline HA coatings on metallic substrates without any post deposition thermal treatment as also showed by some of our previous results [27].

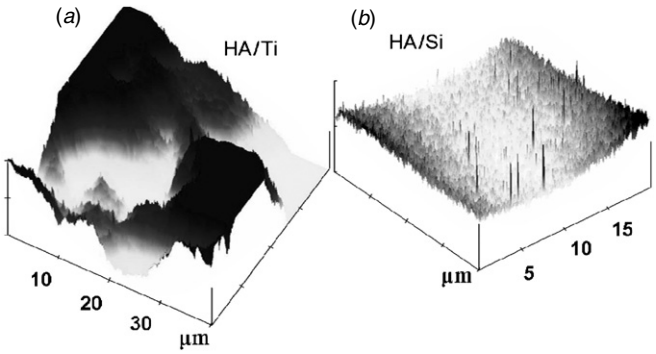

Figure 4. AFM images of as-sputtered HA films for sputtering times of 180 min with 120 W RF power show the surface roughness of (*a*) HA/Ti larger than 1 μm and (*b*) HA/Si around 10 nm.

The film surfaces, on which cells were seeded, figures 4(*a*) and (*b*), are nearly homogeneous with an (root mean square) rms-roughness of about 10 nm for films grown on silicon; a considerably larger roughness is seen when titanium substrates are used. In general, the film morphology follows the texture of the substrate surface. The surface composition of the 180 min films, determined by XPS spectra, showed the calcium, phosphate and oxygen peaks of only a single mineral species and the Ca/P and O/P ratios were close to those for stoichiometric HA (see figure 5). A carbon peak (of inorganic origin) at 285 eV suggests that carbonate was formed on the

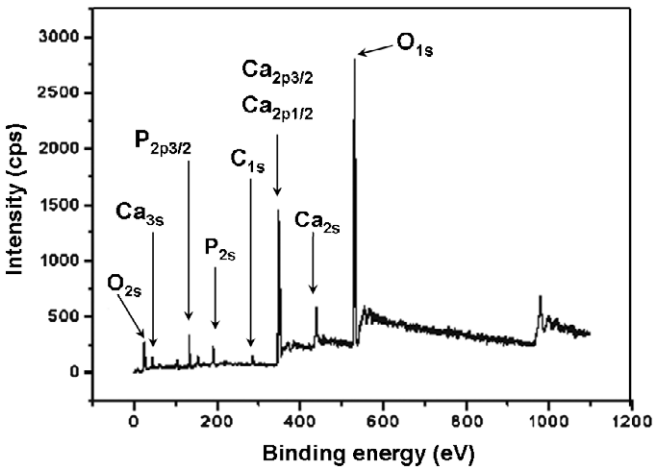

Figure 5. XPS spectrum showing the surface composition and chemical state of the as-sputtered HA/Si film, for sputtering time of 180 min with 120 W RF power.

HA surface when the film was exposed to the atmosphere after removing the samples from the chamber.

3.2. Film behavior in simulated body fluid (SBF)

An as-sputtered calcium phosphate film with controlled stoichiometry, roughness, crystallinity and thickness was immersed in SBF for 10 days. After that time a well-crystallized mineral phase composed of plate-like crystals was formed on the film surface as shown in figure 6. The EDS analysis confirms that those crystals were associated with calcium phosphate. This result agrees with other reports [28, 29].

3.3. Cells culture on HA coated substrates

Osteoblast cells adhesion density, in cells cm^{-2}, for all substrates is illustrated in figure 7. The results obtained from cell adhesion experiments showed greater adhesion of osteoblasts to HA coated titanium and HA coated Si compared to glass reference (figure 7). In addition, osteoblast adhesion was greater on HA coated titanium compared to HA coated Si, which might be attributed to differences in the surface roughness between the coatings. Since adhesion of osteoblast is a prerequisite for their deposition of bone, these results suggest greater long term functions of osteoblast on HA coated titanium.

HA coatings homogeneously distributed over the silicon and titanium substrates, as well as films having special topographies, were also studied in order to assess the osteoblast behavior on both smooth and complex surfaces. For this kind of investigation the RAMS technique is convenient because various coating characteristics such as thickness, roughness and stoichiometry can be easily controlled. We found that murine osteoblast cells are strongly attached to the HA coating and rapidly spread over the surface of the substrates. On Si(0 0 1), where the HA coating was not well bonded to the substrate, it was observed (see figure 8) that the tension produced by cell attachment was so strong that

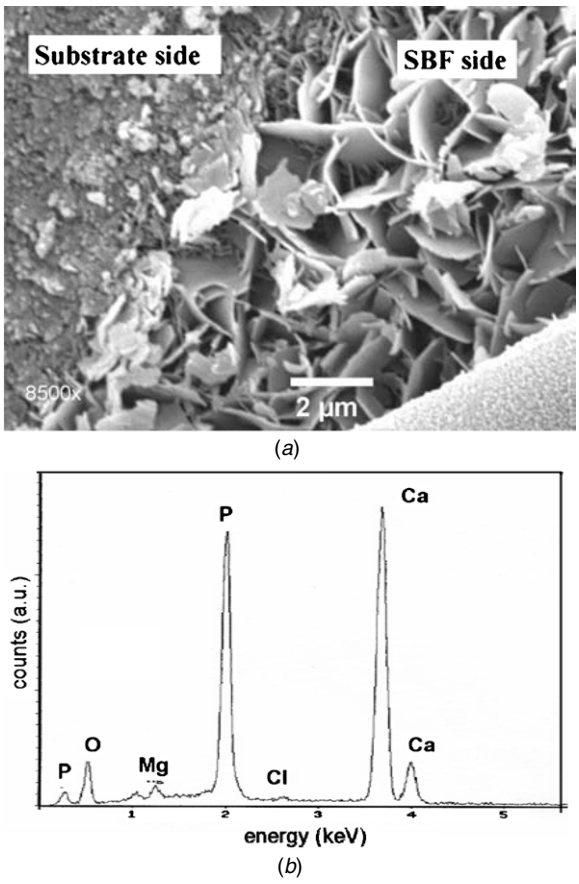

Figure 6. (*a*) Scanning electron micrograph of calcium phosphate crystals precipitated on HA film after immersion in simulated body fluid (SBF) for 10 days. (*b*) EDS analysis of HA film after immersion in SBF for 10 days shows the calcium phosphate nature of crystals precipitated on coating surface.

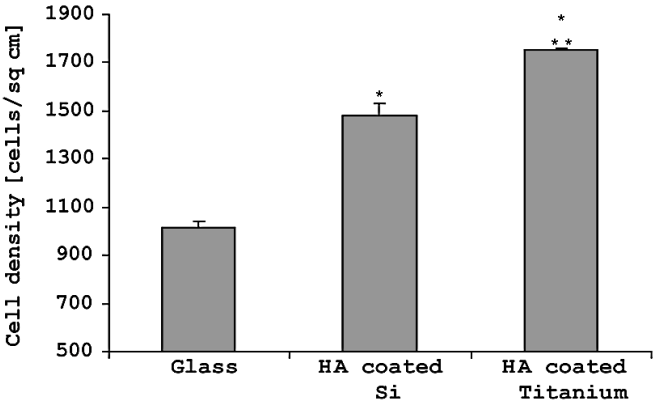

Figure 7. Increased osteoblast cell density on HA coated titanium and HA coated Si by RAMS compared to glass. Values are mean ± SEM; $^{*}p < 0.1$ compared to glass; $^{**}p < 0.1$ compared to HA coating on Si substrate.

the coating detached from the substrate surface at various places. Figures 9(*a*)–(*d*) show some distribution patterns of osteoblast cell growth on a Ti substrate for which half was coated by HA (HA/Ti region) and the other half was uncoated (Ti/Ti). Cells in the Ti/Ti region were usually present in lower concentrations than in the HA/Ti regions (figures 9(*a*) and 9(*b*) respectively). Moreover, the projected area of the

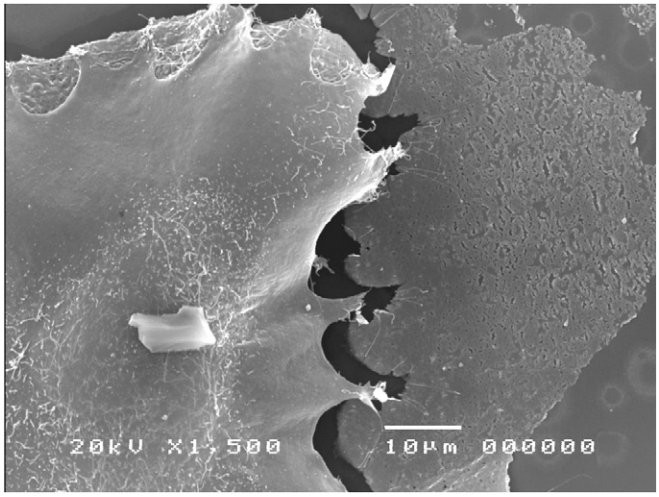

Figure 8. Scanning electron micrograph of HA/Si 4 h after seeding with osteoblast cells showing coating detachment caused by cell tension.

individual cells in the HA/Ti region was smaller, probably due to the higher cellular densities. When looking at the interface between Ti/Ti and HA/Ti, the difference in projected cell areas was evident, with a denser packing of cells in the HA/Ti region (figures 9(*c*) and (*d*)). Right at the interface, a different pattern of cell distribution was also seen (possibly related to the surface topographies and chemistry). Some cells aligned parallel to the separation line at the interface (figure 9(*c*)). Also, we found that the cells are oriented perpendicularly to the interface, in some specific regions of the Ti/Ti, as shown in figure 9(*d*).

3.4. Cell culture studies on engineered HA substrates

3.4.1. The step and groove scaffold. The HA coatings were also deposited over Si(0 0 1) substrates which were machined, using a diamond saw, forming parallel grooves for further cell culture studies (figure 10(*a*)). Just after seeding, most murine osteoblast cells were found at the bottom of the grooves, due to the capillarity effect caused by the step and groove topography (figure 10(*a*)). Cells observed 3 h after seeding mostly remained at the bottom of the grooves. Some cells had already spread out, mainly elongating parallel to the groove axis and along the striations resulting from sawing the grooves; (figure 10(*b*)) a few other cells had a more circular geometry (not shown). After 48 h, a different cell distribution pattern was observed. The scaffold's upper surface (the un-cut Si surface) appeared almost completely covered by cells, with

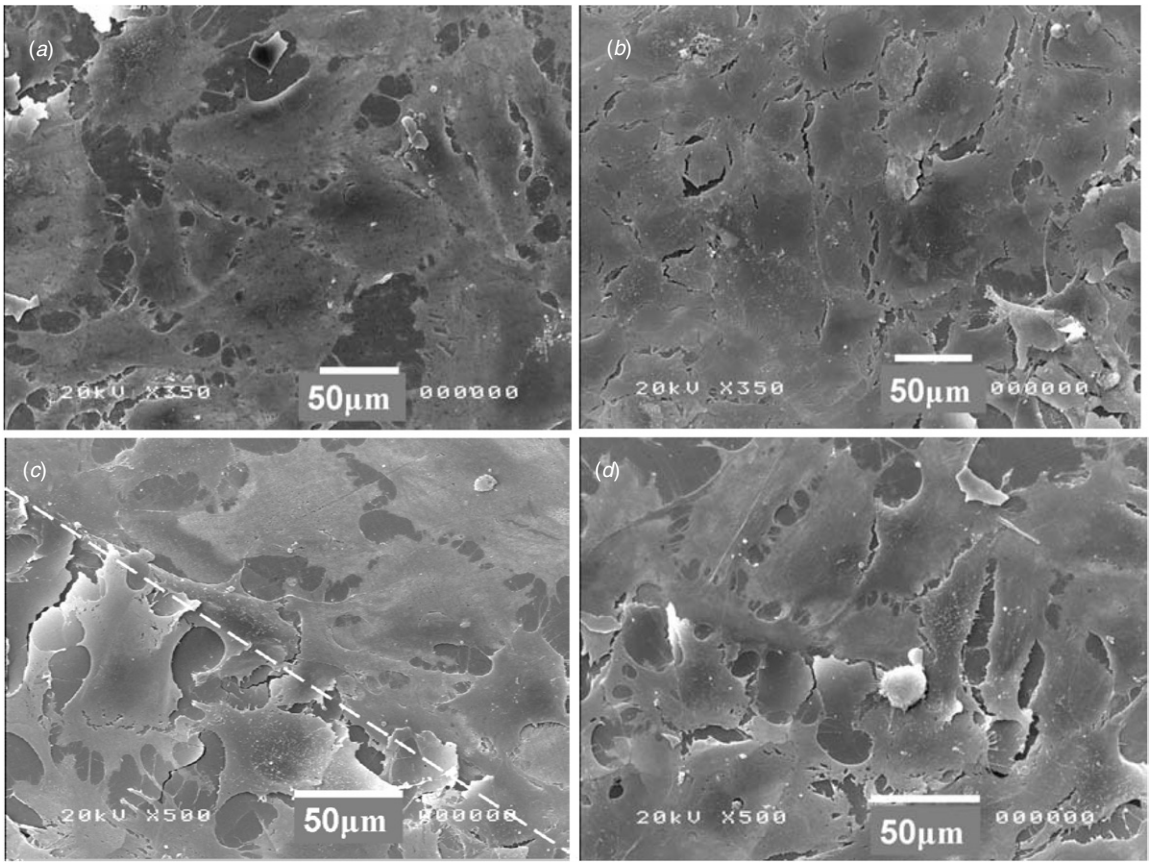

Figure 9. SEM images in the vicinity of the line separating the titanium (Ti/Ti) and HA covered titanium (HA/Ti) regions containing osteoblasts 72 h after *in vitro* seeding. (*a*) Cells on Ti/Ti appeared highly spread, presenting high projected surface areas; (*b*) cells over the HA/Ti region were more densely packed than in the previous surface, and thus presented a lower projected area per cell; (*c*) and (*d*) specific patterning observed near the interface (dashed line) Ti/Ti × HA/Ti, with cells over the Ti/Ti region lining perpendicularly to the HA/Ti covered region. In both figures, a row of cells lying parallel to the interface can be observed.

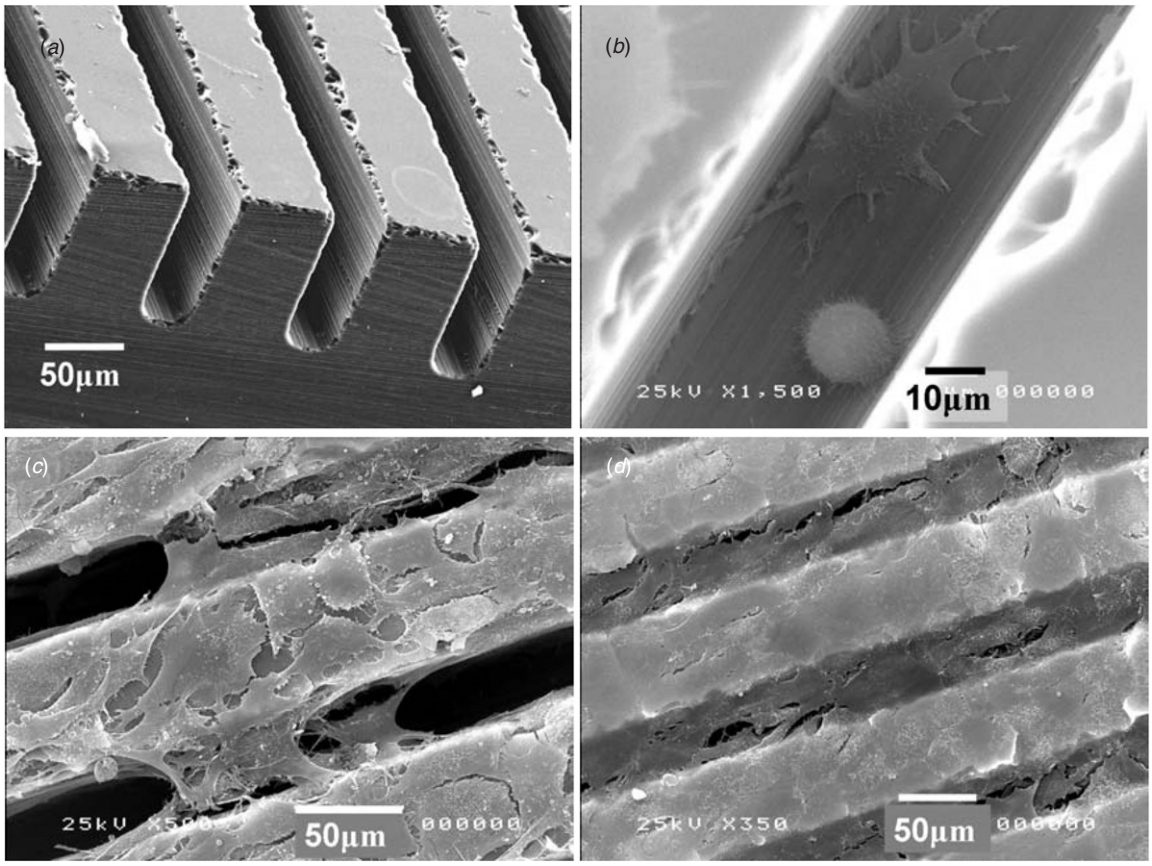

Figure 10. (*a*) SEM images of a HA coated grooved silicon substrate; (*b*) 4 h after seeding with osteoblast cells, where two cells can be seen in the bottom region of the substrate while part of a cell appears at the upper surface (top left in the figure); (*c*) 24 h after seeding with osteoblast cells, the cells were seen mainly on the upper surface of the substrate and formed bridges between the stripes of this surface over the 36 μm gap region. Here, it was possible to observe a cell attached to adjacent vertical walls without contact with the bottom surface; (*d*) 48 h after seeding, osteoblast cells produced a continuous layer at the level of the upper surface of the substrate.

different cell densities. In some areas, it was clearly observed that cells were migrating up the step wall in the direction of the upper surface of the scaffold (figure 10(*c*)). In some cases, it was observed that the cells bridged two of the step walls without touching the bottom of the groove, indicating that they were climbing the two walls simultaneously (figure 10(*c*)). In other regions of the same scaffold, a continuous layer of cells was formed at the upper surface, with the cells forming bridges over the gap caused by the grooves (figure 10(*d*)).

3.4.2. The cylindrical pillars. After HA deposition some Si(0 0 1) substrates were properly photo-lithographically patterned into cylindrical pillars. Murine osteoblast cells seeded on this scaffold rapidly spread across the Si region of the substrate (figure 11(*a*)) in as little as 3 h after seeding. In this case the cells were extremely flat. Cells could also sense the very small step caused by the presence of the very short cylindrical pillars (<1 μm in height) surrounding the pillars (figure 11(*a*) and cell on the left side of figure 11(*b*)). In a second moment cells spread over the cylindrical walls of the pillars (cell on the right side of figure 11(*b*)). Afterwards, cells proliferated and completely covered the pillars (figure 11(*c*)).

Cells are attached firmly to the HA cylindrical pillars, as can be observed in figure 11(*d*) and inset, where the film layer has broken laterally, probably due to tension caused by the cell on spreading. The inset in figure 11(*d*) also suggests that the HA crystallites of the film layer have a columnar structure and are arranged with the [0 0 2] (*c*-axis) direction perpendicular to the substrate surface, since they appear as needle-like structures, all lying parallel with the long axis perpendicular to the surface.

4. Discussion

In this work we produced different calcium phosphate thin coatings using a RAMS technique. This new design permits the production of stoichiometric and crystalline as-sputtered coatings of phase-pure HA, which is apparently not possible with the plasma spray technique or even with conventional magnetron sputtering. The thickness was easily controlled by varying the sputtering time, and crystallinity was dependent on the RF power. For films thinner than 100 nm, high crystallinity and preferential orientation could be obtained with thermal treatment at moderate temperatures up to 500 °C. HA films on Si appear to orient as a consequence of epitaxial growth, with the hydroxyapatite *c* axis being perpendicular to the substrate surface, as shown by the XRD patterns (figure 2). In regions where the HA layer detaches from Si substrate allowing a cross-sectional view to be obtained by SEM

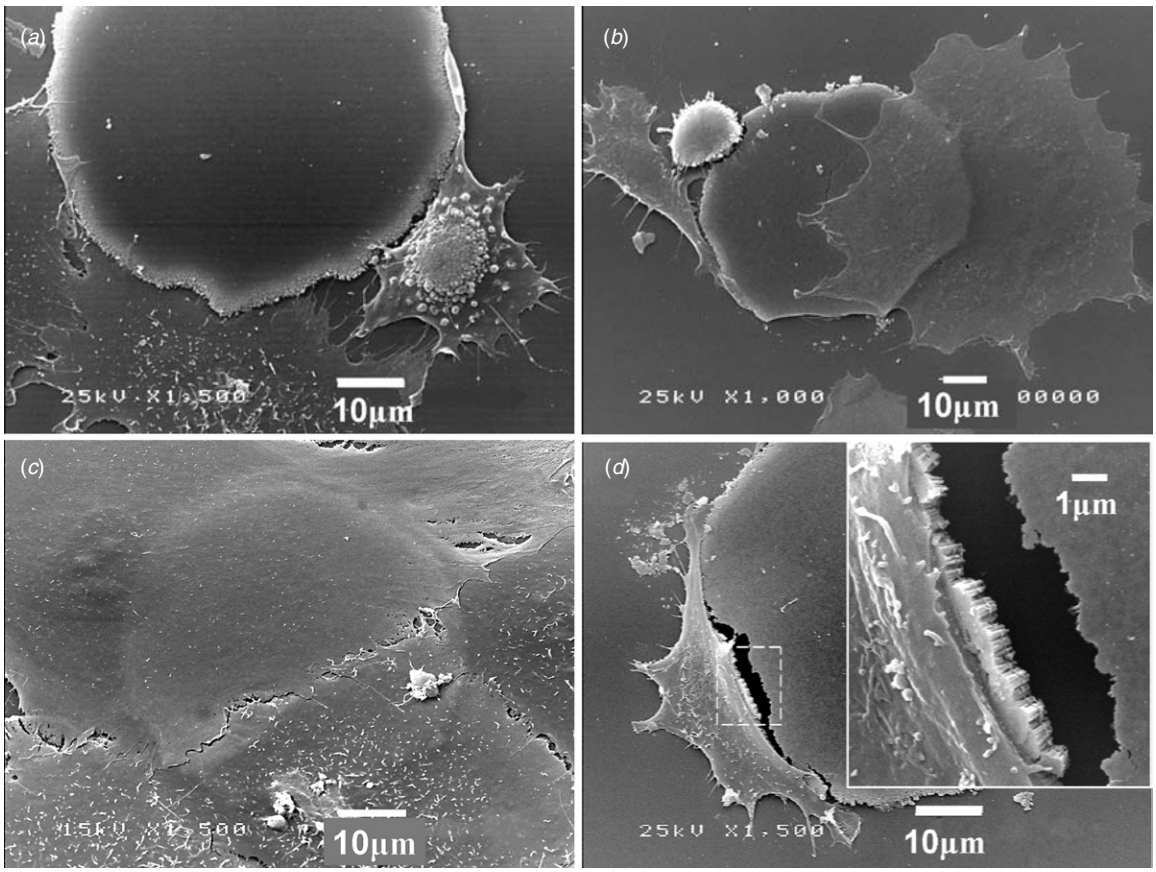

Figure 11. (*a*) Osteoblast cells seeded on silicon substrate containing a short pillar region of HA (of about 1 μm in height). (*b*) An osteoblasts cell on the right side is highly spread over the silicon surface and part of the cell moved to the HA pillar region without discontinuity in the spreading pattern. The cell at the left side in the figure recognized a step over the substrate and appeared to be surrounding the pillar step; (*c*) cells proliferated and completely covered the pillars; (*d*) a broken HA pillar with an osteoblast cell hardly attached to detached coating; in detail, the HA coating broken side view showing a columnar growing structure with the highest dimension oriented perpendicularly to the substrate surface.

(figure 11(*d*)), several needle-like HA crystallites arranged in parallel columns and perpendicular to the surface were seen, which revealed that films had a columnar structure.

The roughness and adhesion to the substrate of the coatings is related to the nature of substrate surface and to the sputtering conditions. In this work, no special roughness was performed onto substrate surfaces by chemical or mechanical treatment, prior to HA deposition, since coating adhesion was not the focus of this investigation. We used smooth and non-porous coatings in order to facilitate: (i) characterization of the coating structure, and (ii) observation of the contact between cell and coating. A detailed study of the conditions that optimize coating adhesion to the substrate is in progress.

Coatings on silicon were smoother and more homogeneous, but showed less adhesion to the substrate than films grown on titanium. The high homogeneity of the HA layer was confirmed by both SEM analysis and the morphology of cells grown over the layers. So, that cells spread homogeneously over the whole layer. However, in some regions the film layer displayed a poorly defined contour (not shown) with the HA layer ending as a wedge, with a less dense material and discontinuities of the HA layer. Also the film layer detached from the substrate in several regions, mainly for the Si substrate large area. This was probably due to the very flat and smooth structure of the silicon substrate and the sample preparations for the SEM analysis. These constraints were not an impediment for the present study as we could observe cells in both the uncovered and sputter-coated regions of the substrates. For the case of Ti, the surface had a higher roughness, which implies that the cells can attach more strongly to the sputtered film layer.

The cells seeded onto HA coated Ti substrates produced by RAMS showed that this technique is more favorable. This result is a strong indication that RAMS has the potential to produce bioactive coatings for biomedical applications. Some challenges for the near future are posed, e.g. optimizing the sputtering parameters and using chemically and/or mechanically treated Ti substrates in order to optimize the coating adhesion to the substrate.

In addition, the production of flat, homogeneous, thin and chemically controlled HA-coated surfaces is essential if one is to carry out controlled *in vitro* studies in which the same topography but chemically different surfaces are studied. The fact that our RAMS produces uniform coatings permits cell density, spreading proliferation, and overall morphology to be easily analyzed for two chemically different substrate surfaces at the same time, under conditions where the same number of cells are seeded. The *in vitro* experiments using

osteoblast cells derived from Balb/c mouse femurs seeded onto Si, Ti and thin HA coatings revealed some interesting examples of cell behavior when in contact to different materials surfaces. The experiments show that osteoblasts have a special behavior on Si surface: they rapidly adhere and spread over the surface, becoming very flat following the surface morphology. These results may suggest a high surface wettability for Si as previously shown by others [30]. The strength of osteoblast interaction with the material surface could be observed when cells were seeded on an HA film surface; SEM images show that in some cases even when the film has broken, cells became attached to the coating, showing the strong mechanical forces exerted by cells at the adhesion regions (figure 8). In other situations, it seems that the cell creates enough stress to detach the film and break it (figure 11(*d*)). When cells are in contact with a complex scaffold, such as a Si groove pattern, they can easily migrate from the bottom (not coated with HA) to the top of the groove (coated with HA) by crawling two walls simultaneously.

5. Conclusions

A RAMS system has been shown to produce crystalline HA thin coatings without the need for *in situ* or *ex situ* annealing. *In vitro* cell culture studies have demonstrated that the as-sputtered HA coatings promote the growth of osteoblast cells. Cells attached to all coated surfaces, and experienced a continuous change in surface morphology as they proliferated with time, presenting specific morphological patterns in the different surfaces and interfaces. In summary, this result suggests that RAMS may be a promising alternative to the plasma spray technique for depositing HA coatings on metallic implants, in addition to being a good model for *in vitro* studies on the interaction of osteoblast cells with bioceramic surfaces.

Acknowledgments

This work was supported by the US National Science Foundation under Grant DMR-0303491 and through the Projeto-CIAM-CNPq, Brazil. The authors thank Dr Guinter at the Brazilian Synchrotron Laboratory and Leonardo R Andrade from the *Laboratório de Biomineralização* at Federal University of Rio de janeiro, for the help with electron microscopy imaging and its analysis.

References

[1] Katti S K 2004 Biomaterials in total joint replacement *Colloids Surf.* B **39** 133–42
[2] Brunette D M, Tengvall P, Textor M and Thomsen P 2001 *Titanium in Medicine* (Berlin: Springer)
[3] Bagno A and Bello D C 2004 Surface treatments and roughness properties of Ti-based biomaterials *J. Mater. Sci. Mater. Med.* **15** 935–49
[4] Vanzillotta P S, Sader M S, Bastos I N and Soares G D A 2006 Improvement of *in vitro* titanium bioactivity by three different surface treatments *Dent. Mater.* **22** 275–82
[5] Ong J L and Chan C N 1999 Hydroxyapatite and their use as coatings in dental implants: a review *Crit. Rev. Biomed. Eng.* **28** 667–707
[6] Herman H 1988 Plasma spray deposition processes *Mater. Res. Soc. Bull.* **12** 60–7
[7] Uchida M, Oyane A, Kim H-M, Kokubo T and Ito A 2004 Biomimetic coating of laminin-apatite composite on titanium metal and its excellent cell-adhesive properties *Adv. Mater.* **16** 1071–4
[8] Narayanan R, Seshadri S K, Kwon T Y and Kim K H 2007 Electrochemical nano- grained calcium phosphate coatings on Ti-6Al-4V for biomaterial applications *Scr. Materialia* **56** 229–32
[9] Padilla S, Roman J, Carenas A and Vallet-Regi M 2005 The influence of the phosphorus content on the bioactivity of sol-gel glass ceramics *Biomaterials* **26** 475–83
[10] Choi J-M, Kim H-E and Lee I-S 2000 Ion-beam-assisted deposition (IBAD) of hydroxyapatite coating layer on Ti-based metal substrate *Biomaterials* **21** 469–73
[11] Rabiei A, Thomas B, Jin C, Narayan R, Cuomo J, Yang Y and Ong J L 2006 A study on functionally graded HA coatings processed using ion beam assisted deposition with *in situ* heat treatment *Surf. & Coat. Technol.* **200** 6111–6
[12] Lee I-S, Kim D-H, Kim H-E, Jung Y-C and Han C-H 2002 Biological performance of calcium phosphate formed on commercially pure Ti by electron-beam evaporation *Biomaterials* **23** 609–15
[13] Nelea V, Morosanub C, Iliescuc M and Mihailescud I N 2004 Hydroxyapatite thin films grown by pulsed laser deposition and radio-frequency magnetron sputtering: comparative study *Appl. Surf. Sci.* **228** 346–56
[14] Yang Y, Kim K-H and Ong J L 2005 A review on calcium phosphate coatings produced using a sputtering process—an alternative to plasma spraying *Biomaterials* **26** 327–7
[15] Jansen J A, Wolke J G C, Swann S, van der Waerden J P and de Groot K 1993 Application of magnetron sputtering for the producing ceramic films on implant materials *Clin. Oral Implant Res.* **4** 28–34
[16] Hulshoff J E G, van Dijk K, van der Waerden J P, Wolke J G C, Ginsel L A and Jansen J A 1995 Biological evaluation of the effect of magnetron sputtered Ca/P films on osteoblast-like cells *in vitro J. Biomed. Mater. Res* **29** 967–75
[17] van Dijk K, Schaeken H G, Wolke J G C and Jansen J A 1996 Influence of annealing temperature on RF magnetron sputtered calcium phosphate films *Biomaterials* **17** 405–10
[18] Ong J L and Lucas L C 1994 Post-deposition heat treatment for ion beam sputter deposited calcium phosphate films *Biomaterials* **15** 337–41
[19] Yang Y, Kim K, Agrawal C M and Ong J L 2003 Effect of postdeposition heating temperature and the presence of water vapor during heat treatment on crystallinity of calcium phosphate films *Biomaterials* **24** 5131–7
[20] Thian E S, Huang J, Best S M, Barber Z H and Bonfield W 2005 Magnetron co-sputtered silicon-containing hydroxyapatite thin films—an *in vitro* study *Biomaterials* **26** 2947–56
[21] Wolke J G C, de Groot K and Jansen J A 1998 *In vivo* dissolution behavior of various RF magnetron sputtered Ca-P films *J. Biomed. Mater. Res.* **39** 524–30
[22] Zheng J Q, Shih M C, Wang X K, Williams S, Dutta P, Chang R P H and Ketterson J B 1991 A miniature x-ray compatible sputtering system for studying *in situ* high T_c thin film growth *J. Vac. Sci. Technol.* A **9** 128–32
[23] Morita Y and Nishizawa M 2005 Surface preparation of Si.001 substrate using low-pH HF solution *Appl. Phys. Lett.* **86** 171907
[24] Hong Z, Luan L, Paik S B, Deng B, Ellis D E, Ketterson J B, Mello A, Eon J G, Terra J and Rossi A 2007 Crystalline hydroxyapatite thin films produced at room temperature—an opposing radio frequency magnetron sputtering approach *Thin Solid Films* at press

[25] Takadama H, Hashimoto M, Mizuno M, Ishikawa K and Kokubo T 2004 Newly improved simulated body fluid *Key Eng. Mater.* **254–256** 115–8

[26] Balduino A, Hurtado S P, Frazão P, Takiya C M, Alves L M, Nasciutti L E, El-Cheikh M C and Borojevic R 2005 Bone marrow subendosteal microenvironment harbours functionally distinct haemosupportive stromal cell populations *Cell Tissue Res.* **319–2** 255–66

[27] Hong Z *et al* 2007 Characterization of crystalline hydroxyapatite thin coatings for biomedical applications *Key Eng. Mater.* **330–332** 525–8

[28] Wolke J G C, de Groot K and Jansen J A 1998 Dissolution and adhesion behaviour of rf magnetron sputtered CaP films *J. Mater. Sci.* **33** 3371–6

[29] Boyd A R, Meenan B J and Leyland N S 2006 Surface characterization of the evolving nature of radio frequency (RF) magnetron sputter deposited calcium phosphate thin films after exposure to physiological solution *Surf. & Coat. Technol.* **200** 6002–13

[30] Thian E S, Huang J, Best S M, Barber Z H and Bonfield W 2007 Surface wettability enhances osteoblasts adhesion on silicon-substituted hydroxyapatite thin films *Key Eng. Mater.* **330–332** 877–80